Determining Accurate Kinetic Parameters of Potentially Important Heterogeneous Atmospheric Reactions on Solid Particle Surfaces with a Knudsen Cell Reactor

G. M. Underwood, P. Li, C. R. Usher, and V. H. Grassian*

Department of Chemistry and Center for Global and Regional Environmental Research, University of Iowa, Iowa City, Iowa 52242

Received: August 25, 1999; In Final Form: October 20, 1999

One of the most important applications of the Knudsen cell reactor is in determining heterogeneous reaction kinetics of potentially important atmospheric reactions. Knudsen cell measurements involving gas reactions on atmospherically relevant particle surfaces, including salt, carbon black, soot, and mineral dust, are often obtained using powdered samples. In this study, we have investigated the importance of gas diffusion into the underlying layers of powdered samples when determining kinetic parameters from Knudsen cell experiments. In particular, we show that the use of the geometric surface area of the sample holder is, in general, not justified in determining initial uptake coefficients or reaction probabilities because the interrogation or probe depth of gas-phase molecules into the bulk powder can be anywhere from tens to thousands of layers deep. One problem encountered by current models used to account for gas diffusion into the underlying layers is that the diffusion constant of the gas through the powdered sample must be known. Typically, diffusion constants for gases into powdered samples are unknown and are difficult to measure or accurately calculate. One way to circumvent this problem is to use thin samples such that the thickness of the sample is less than the interrogation depth of the gas-phase molecules. Under these conditions, the observed initial uptake coefficient is directly proportional to the surface area of the entire sample. This region is termed the linear mass-dependent regime and can be experimentally accessed for many, but not all, heterogeneous reactions. Several examples discussed here include heterogeneous reaction of NO_2 on γ- and α-Al_2O_3, α-Fe_2O_3, carbon black; HNO_3 on $CaCO_3$; and acetone on TiO_2.

Introduction

The use of the Knudsen cell, a very low-pressure flow reactor, to obtain kinetic information for heterogeneous gas−solid and gas−liquid reactions was pioneered over 30 years ago by Golden, Spokes, and Benson.[1] The technique is ideally suited for the study of heterogeneous reactions in that at the experimental pressures used, the mean free path of the molecules in the cell usually exceeds the dimensions of the cell. This minimizes the possibility of gas-phase collisions and eliminates boundary layer effects, which greatly simplifies the analysis of the data. In addition, the technique has a wide dynamic range with the ability to measure reaction probabilities from near unity to 10^{-7}.[2] For these reasons, Knudsen cell reactors have become, in many ways, a workhorse for obtaining heterogeneous kinetic data for a wide variety of chemical systems pertaining to catalysis[3] and atmospheric chemistry.[4,5]

In the past few years, however, there has been some controversy in the literature as to the applicability of the simple analysis typically used to determine heterogeneous uptake coefficients[6] from Knudsen cell data, especially for experimental systems in which the reactive surface consists of multiple layers of porous[7−10] or powdered samples.[11−14] The controversy arises from the use of the geometric area of the sample holder in the analysis of the data, as opposed to a multiparticle surface area that allows for gas diffusion into the interstitial pores between the particles. Recently, it was demonstrated that for NO_2 reacting with relatively thin samples of mineral oxide particles in a Knudsen cell reactor, the entire BET surface area is accessible for adsorption and reaction over the course of the experiment.[14] However, correcting the observed uptake coefficient, in particular the initial uptake coefficient, for this increased surface area requires an understanding of how much of the powdered sample is probed by the gas phase during the time scale of the measurement.

In 1991 Keyser, Moore, and Leu (KML) proposed a semiempirical model to account for gas diffusion into porous samples. In the KML model, an "effectiveness factor" was determined to account for the contribution of underlying layers to the observed uptake coefficient measured with a flow tube reactor.[7] Importantly, the model correctly reproduced the mass dependence of the observed uptake coefficient for the reaction of $ClONO_2$ with HNO_3−H_2O ice and demonstrated that the internal structure can contribute significantly to the reactive surface area. Since then, there have been disagreements in the literature pertaining to the KML model as it applies to the reaction of N_2O_5 and $ClONO_2$ on ice films.[8−10] However, the consensus reached seems to be that it is due to a lack of adequate characterization of the ice films rather than any flaw in the model.[9,10]

In 1996, Fenter, Caloz, and Rossi adopted the KML model for Knudsen cell studies of N_2O_5 and HNO_3 on salt particles (NaCl and KBr) with varied degrees of success.[11] The model not only produced the observed mass dependence for the heterogeneous uptake coefficient of N_2O_5 on salt but also correctly showed that the kinetic limit is reached with less sample mass for smaller grain size. However, the model did

* To whom correspondence should be addressed.

10.1021/jp9930292 CCC: $19.00
Published on Web 01/05/2000

not fit their HNO_3 data, which showed no mass dependence for the observed initial uptake coefficient. It is likely that the model failed because it assumes the diffusion constant can be calculated from a simple diffusion equation, which assumes ideal gas behavior (vide infra). There are no provisions in the model for the reduction in the diffusion constant, which would certainly occur for a "sticky" molecule like HNO_3. Finlayson-Pitts and Biechert have also studied the reaction of HNO_3 on NaCl and found no mass dependence.[13] However, the presence of a strongly adsorbed water layer caused an initial spike in their uptake data, so reaction probabilities from later times in the experiment, where the rate of change was smaller, were reported. The flux of molecules to the surface was also varied with the sample mass. Although there may indeed be no observable mass dependence for the range of masses studied, several factors could hinder the interpretation of the Knudsen cell data for this reaction. These factors include a lack of information on the real diffusion constant, delayed determination of the uptake coefficient, variable pressures used in the experiments, and the amount of water present on the salt particle surface.

The purpose of this study is to consider and to some extent deconvolute the experimental factors that may be responsible for the apparent failure of the KML model in some cases. For example, the heterogeneous uptake coefficient measured for NO_2 on carbon black is reported to have no dependence on the mass of the carbon black sample.[12] However, an analysis of the NO_2 carbon black system shows that the mass dependence is limited to extremely thin samples that would be exceedingly difficult to prepare in the laboratory (vide infra). It is important to note that in many published studies it is impossible to determine whether there is a mass dependence and if the KML model is applicable because the mass of the powdered samples is not reported.

In addition to presenting a comprehensive discussion of the application of the KML model to gas reactions on powdered samples, we will demonstrate that the linear mass dependence (LMD) regime can be used to analyze the Knudsen cell data for powdered samples. This analysis does not require any knowledge of the diffusion constant of the gas in the powdered sample. In the LMD regime, only the total mass of the particles and the BET surface area of the particles need to be measured.

Experimental Section

A Knudsen cell reactor coupled to a quadrupole mass spectrometer (UTI, DetecTorr II) is used to determine uptake coefficients on powdered samples. The mass spectrometer is housed in a vacuum chamber equipped with a 400 L/s ion pump and an ion gauge (both from Varian). The region between the quadrupole mass spectrometer and the Knudsen cell reactor is pumped by a 150 L/s turbomolecular pump (Leybold) for differential pumping of the mass spectrometer.

The Knudsen cell reactor consists of a stainless steel reducing cross with a sample holder attached to the bottom flange. The area of the sample holder, A_s, is 11.88 cm^2. For most experiments, all exposed interior surfaces are either coated with Teflon or Halocarbon Wax series 1500 to provide a chemically inert surface. A blank flange attached to a linear translator serves as a cover for the powdered sample. The seal between the sample holder and the cover is made with a viton O-ring.

The cell volume and escape constant were determined by monitoring the pressure in the cell as a function of time after steady-state flow into the cell was abruptly stopped. For these experiments the natural log of the relative pressure as a function of time yields a slope equal to the negative of k_{esc}. This value can in turn be used to determine the cell volume through the equation

$$k_{esc} = \frac{\upsilon A_h}{4V} \quad (1)$$

where υ is the average gas-phase velocity, A_h is the effective area of the escape aperture accounting for the Clausing factor, and V is the volume of the cell. By use of an aperture of 0.0204 cm^2 with a Clausing factor of 0.4726,[15] the escape constant and cell volume were determined to be 0.12 s^{-1} and 765 cm^3, respectively.

Samples for the Knudsen cell were prepared in one of two ways depending on how much sample was required for the experiment. For relatively large amounts of sample, typically 0.5−2.0 g, the powdered sample was spread evenly across the sample holder and then lightly pressed down to form a flat surface. When much less sample, approximately 2−100 mg, was needed, the powder was sprayed onto the sample holder. It is very important, for thin samples, that the powdered sample be evenly applied and it must cover the entire geometric area of the sample holder; otherwise, the initial uptake coefficient may reflect the amount of uncovered/unreactive surface in the sample holder as well as the sample mass. Both of these concerns are addressed by using an atomizer to spray an aqueous slurry of the sample onto a heated sample holder. This spraying procedure ensured very even coverages of the powdered sample across the bottom of the sample holder, as determined with an optical microscope.

For all Knudsen cell experiments, flowing the reactive gas through the reactor for at least 90 min prior to the experiment passivated the walls of the reactor. The gas was introduced through a leak valve to the desired pressure as measured with an absolute pressure transducer (MKS 690A.1TRC, range 10^{-6}−0.1 Torr). During passivation the powdered sample was sealed with the blank flange.

NO_2 (Matheson, 99.95% minimum purity) was used as received. The acetone vapor was taken from a liquid acetone sample (Fisher Scientific HPLC Grade, 99.6% purity) that was subjected to several freeze−pump−thaw cycles each day prior to use. Dry gaseous nitric acid was taken from the vapor of a 1:3 mixture of concentrated HNO_3 (70.6% HNO_3, Mallinckrodt) and H_2SO_4 (95.9%, H_2SO_4, Mallinckrodt). The powdered samples used in these experiments were obtained from commercial sources. The source and relevant physical properties for each sample are given in Table 1. Bulk densities were determined by filling the sample holder of known area with powder to a given depth and weighing the amount of sample that occupied this volume. BET surface areas of the powdered samples were determined from a multipoint BET analysis (Quantochrome Nova 1200).

Background Information for Determining Heterogeneous Kinetic Parameters from Knudsen Cell Data

Derivation of the Uptake Coefficient for Heterogeneous Reactions. The general design of Knudsen cell reactors for the study of heterogeneous reactions has been described in detail in the literature.[1,2,4] Briefly, the reactor consists of a chamber with an isolated sample compartment and a small orifice through which gas-phase reactant and product species can escape and be detected, usually by mass spectrometry. In a typical Knudsen cell experiment, the sample compartment is covered while the

TABLE 1: Physical Properties of Powdered Samples and Parameters Used to Calculate γ_t

parameter	symbol	γ-Al_2O_3	α-Al_2O_3	α-Fe_2O_3[a]	C-black	TiO_2	$CaCO_3$
source		Degussa (Aluminumoxid C)	Aesar (39814)	Aldrich (310005-0)	Degussa (FW2)	Degussa (P25)	Aldrich (20293-2)
diameter	d	1.8×10^{-6} cm	1.0×10^{-4} cm	6.9×10^{-5} cm	1.3×10^{-6} cm	2.5×10^{-6} cm	3.5×10^{-4} cm
surface area	S_{BET}	1.0×10^{6} cm^2/g	1.4×10^{5} cm^2/g	1.8×10^{4} cm^2/g	4.6×10^{6} cm^2/g	5.0×10^{5} cm^2/g	1.4×10^{4} cm^2/g
true density	ρ_t	3.7 g cm^{-3}	4.0 g cm^{-3}	5.24 g cm^{-3}	1.9 g cm^{-3}	4.17 g cm^{-3}	2.93 g cm^{-3}
bulk density	ρ_b	0.15 g cm^{-3}	0.60 g cm^{-3}	1.1 g cm^{-3}	0.16 g cm^{-3}	0.17 g cm^{-3}	0.96 g cm^{-3}
porosity	θ[b]	0.96	0.85	0.79	0.91	0.96	0.67
external height	h_e[c]	2.1×10^{-6} cm	7.6×10^{-5} cm	4.7×10^{-5} cm	1.2×10^{-6} cm	2.9×10^{-6} cm	2.0×10^{-4} cm
sample height (cm/mg)	h_t[d]	5.6×10^{-4}	1.4×10^{-4}	1.8×10^{-4}	5.3×10^{-4}	5.0×10^{-4}	8.8×10^{-5}
number of layers per mg	L[e]	133	0.93	1.9	221	85	.22
surface area per layer	S_L	7.6 cm^2	150 cm^2	9.4 cm^2	21 cm^2	5.9 cm^2	64 cm^2

[a] Experiments with α-Fe_2O_3 were done using a geometric sample holder with area = 5.0 cm^2. All others were done with a larger sample holder as described in the Experimental Section. [b] $\theta = 1 - (\rho_b/\rho_t)$. [c] $h_e = 0.5(\text{particle mass}/\rho_b)^{1/3}$ = one-half the height of one layer. [d] $h_t = [1/(A\rho_b)]$:$h_i = h_t - h_e$. [e] $L = h_t/(2h_e)$.

walls of the reactor are passivated and a steady-state flow is established. Usually the pressure in the cell is kept low enough such that the mean free path of the molecules within the cell is greater than the cell dimensions so that boundary layer effects and homogeneous gas-phase collisions are minimized and can be neglected. The cell can be used at higher pressures, but to ensure molecular flow, the mean free path must be at least a factor of 10 greater than the diameter of the exit orifice.[1]

The equation usually used to analyze Knudsen cell data can be derived by first considering the gas−surface collision frequency, ω, which is given by the kinetic theory of gases as

$$\omega = \frac{\upsilon A}{4}\left(\frac{n}{V}\right) \tag{2}$$

where υ is the average molecular speed, A is the area that the flux of molecules impinges upon, and (n/V) is the number density of the reactant gas. In turn, the number density within the Knudsen cell is a function of the average molecular speed, the flow of molecules out of the cell, F, and the area of the exit aperture, A_h:

$$\frac{n}{V} = \frac{4F}{A_h \upsilon} \tag{3}$$

To determine the flux of molecules to the sample in a Knudsen cell, A is the geometric area of the sample holder, A_s. Substituting this and eq 3 into eq 2 gives

$$\omega = \frac{FA_s}{A_h} \tag{4}$$

It is useful to determine the uptake coefficient, γ, which is simply a measure of how likely the molecule will be taken up by the surface, through either adsorption or reaction, on a per collision basis. It is defined by eq 5:

$$\gamma = \frac{\text{number of molecules lost from the gas phase per second}}{\text{total number of gas−surface collisions per second}} \tag{5}$$

Knudsen cells can be designed so that there is minimal volume change when the sample compartment is opened. In addition, since the flow of molecules into the cell does not change when the sample compartment is opened, the number of the reactant molecules that is "lost" to the surface is equal to the change in flow out of the cell, $(F_o - F)$, where F_o and F represent the gas-phase flow out of the cell with the sample covered and exposed, respectively. When this is combined with eq 4, it is possible to rewrite eq 5 as

$$\gamma = \frac{A_h}{A_s}\left(\frac{F_o - F}{F}\right) \tag{6}$$

Equation 6 is the standard Knudsen cell equation for determining heterogeneous uptake coefficients and reaction probabilities. Since the measured quantity is usually the mass spectral intensity of the reactant gas and this value is directly proportional to the flow out of the cell, eq 6 usually appears in the literature as

$$\gamma = \frac{A_h}{A_s}\left(\frac{I_o - I}{I}\right) = \gamma_{obs} \tag{7}$$

Here, I_o and I are the mass spectral intensities measured with the sample covered and exposed, respectively. For the purposes of this paper, the uptake coefficient calculated using eq 7 will be referred to as the observed uptake coefficient, γ_{obs}.

It is informative to consider the assumptions inherent in deriving eq 6. In setting eq 2, which gives the flux of molecules to the sample area, equal to the total number of gas−surface collisions, it is assumed that each time a gas-phase molecule approaches the sample it collides only once and only with the top layer. If the sample were a liquid or a single crystal or even a porous sample with an uptake coefficient approaching unity, this assumption probably would not introduce any substantial error. However, for porous samples with uptake coefficients much less than unity, both of these assumptions are clearly oversimplifications whose effects must be carefully considered if true uptake coefficients are to be extracted from the data.

Reactant Flux to the Sample. A consideration sometimes ignored in the analysis of Knudsen cell data is that of site blocking. If the impingement rate of the reactant molecules is too high, the incoming gas molecules may start to saturate the limited number of reactive sites before the first data point is collected; this is especially true when γ is high. If the reacted sites passivate the surface to further reaction, the measured uptake coefficient will be artificially lowered because the measured value for γ will reflect collisions with both active (empty) sites and occupied sites. If the occupied sites can undergo further reaction, the subsequent reaction will almost certainly have a different uptake coefficient. As such, the measured value will be skewed to higher or lower values depending on the relative values of the two uptake coefficients. In either case, the effect will be manifest as a pressure dependence in the observed uptake coefficient. This "limited

accommodation" effect can be avoided experimentally by reducing the impingement rate (or pressure), by reducing the data acquisition time, or by a combination of the two. Of course, there is a trade-off here in that as the pressure is reduced, so does signal intensity, and thus, a compromise must be struck to achieve reasonable signal-to-noise levels.

In fundamental studies of sticking coefficients on single-crystal surfaces in ultrahigh vacuum, site blocking effects can be avoided by limiting the number of reactant molecules colliding with the sample.[16] Over the time period of a single data acquisition point, less than 10% of the total number of surface sites should be occupied.[16] For a 10 cm^2 sample, the number of surface sites available for reaction is ($\sim 5 \times 10^{14}$ sites/cm^2)(10 cm^2) = 5×10^{15} sites and the data acquisition time is approximately 0.5 s. This impingement rate would be $(0.1)(5 \times 10^{15})/0.5 = 10^{15}$ molecules/s. This impingement rate corresponds to a maximum pressure of $\sim 3\ \mu$Torr as determined from eq 2 and ideal gas behavior. This calculation is based on an assumed uptake coefficient of 1.0; a lower value would both fill the available sites more slowly and yield a greater effective diffusion coefficient, which would allow the reactant to probe a greater number of surface sites. As a result, for a given sample/reactant combination, the upper limit of the impingement rate is likely to be greater than the value resulting from the simple calculation above. However, if the chemistry is mediated by defect sites, the active site density will be substantially lower than 5×10^{14} sites/cm^2 and the impingement rate will need to be reduced to avoid the effects of limited accommodation. Thus, unless the microscopic details of the reaction are known, the maximum impingement rate that will yield a pressure-independent uptake coefficient will have to be experimentally determined. If that value cannot be determined or cannot be reached experimentally or if the environmentally relevant pressure of the reactant gas is greater than that value, then the pressure dependence should be considered before the reported values are incorporated into atmospheric chemistry models.

KML Model for Heterogeneous Reactions on Porous Samples. As already mentioned above, Keyser, Moore, and Leu (KML) developed a model that attempts to correct uptake coefficients, measured using a geometric area, for gas-phase diffusion into the bulk of the sample.[7] Their work presents a very complete set of justifications and derivations of the equations used in formulating the model. As such, the following is only intended as a brief conceptual overview.

The premise of the model is that the true uptake coefficient, γ_t, can be separated into external and internal components that are related to the observed uptake coefficient, γ_{obs} by the following equation,

$$\gamma_{obs} = \gamma_t\left(\frac{S_e + \eta S_i}{A_s}\right) \tag{8}$$

where the parenthetic term is a correction factor for the effect of gas-phase diffusion into the underlying layers. S_e and S_i are the internal and external surface areas, A_s is the sample holder geometric area, and η is an effectiveness factor. The effectiveness factor is essentially the fraction of the internal surface area that contributes to the measured value of the uptake coefficient. It implies that there is a "probe depth" that the reactant molecules are able to penetrate on the data acquisition time scale. Its value can be calculated from the following equations,

$$\eta = \frac{1}{\phi}\tanh(\phi) \tag{9}$$

$$\phi = \left(\frac{m}{\rho_b A_s d}\right)\left(\frac{3\rho_b}{\rho_t - \rho_b}\right)\left(\frac{3\tau\gamma_t}{4 - 2\gamma_t}\right)^{1/2} \tag{10}$$

where the Thiele modulus, ϕ, is a measure of the relative rates of surface reaction and diffusion into the underlying layers. The value for the Thiele modulus is dependent on the sample mass m, bulk density ρ_b, and particle diameter d, as well as the sample holder geometric area the porous or powdered sample occupies, A_s, and the true uptake coefficient, γ_t. For the experiments described here, the only experimental variable in eq 10 changed is that of mass.

The quantity τ, the tortuosity factor, enters into eq 10 through the equation for the effective diffusion constant, D_e, which is related to the Knudsen diffusion constant D_K as follows,

$$D_e = \frac{\theta D_K}{\tau} \tag{11}$$

$$D_K = \frac{2r_p v}{3} \tag{12}$$

where θ is the porosity of the sample ($\theta = 1 - \rho_b/\rho_t$), r_p is the pore radius, and, as before, v is the average gas-phase molecular velocity. Equation 12 is derived by assuming diffusion through a long straight capillary. The tortuosity is necessary to account for inhomogenieties in the interparticle voids that make the real pore geometry much more complex. Models of porous solids have predicted τ values ranging from 1 to 8; however, most porous solids are not characterized well enough for a reliable calculation to be made and τ must be experimentally determined.[17−20] In addition, Knudsen diffusion assumes elastic collisions between gas-phase molecules and the particles in the powder, and because there is no provision for nonideal gas behavior, it clearly overestimates the diffusion constant for sticky molecules. In these cases, as will be shown, apparent τ values much greater than 8 are used as a way in which to lower the diffusion constant to more realistic values to fit the experimental data.

The appearance of eq 10 is somewhat modified from its form in Keyser et al.[7] in that here we did not assume either simple cubic or hexagonal close-packed spheres. Instead, the experimentally measured bulk density was used in the calculations. In addition the specific surface area was measured rather than calculated. Rewriting eq 8 in terms of measured bulk density and BET surface area yields[7]

$$\gamma_{obs} = \gamma_t \rho_b S_{BET}(h_e + \eta h_i) \tag{13}$$

where S_{BET} is the BET specific surface area, h_e is the height of the first layer, and h_i is the height of all the internal layers calculated from the total mass, the measured bulk density, and the particle mass. Since γ_t also appears in the equation for η, eq 13 must be iteratively solved.

One of the major drawbacks of the KML model is that diffusion constants for reactive gases through powdered samples are difficult to measure and must be calculated using eqs 11 and 12, which makes τ an additional fitting parameter. Strictly speaking, the tortuosity, τ, should be constrained to values from 1 to 8 and is a measure of the complexity of the pore structure of the sample. For the purposes of this paper, τ was used as a parameter to adjust D_e for other physical phenomena such as nonzero residence time or particle morphology. In this way, reduced D_e values are mimicked in the model by increasing the value of τ.

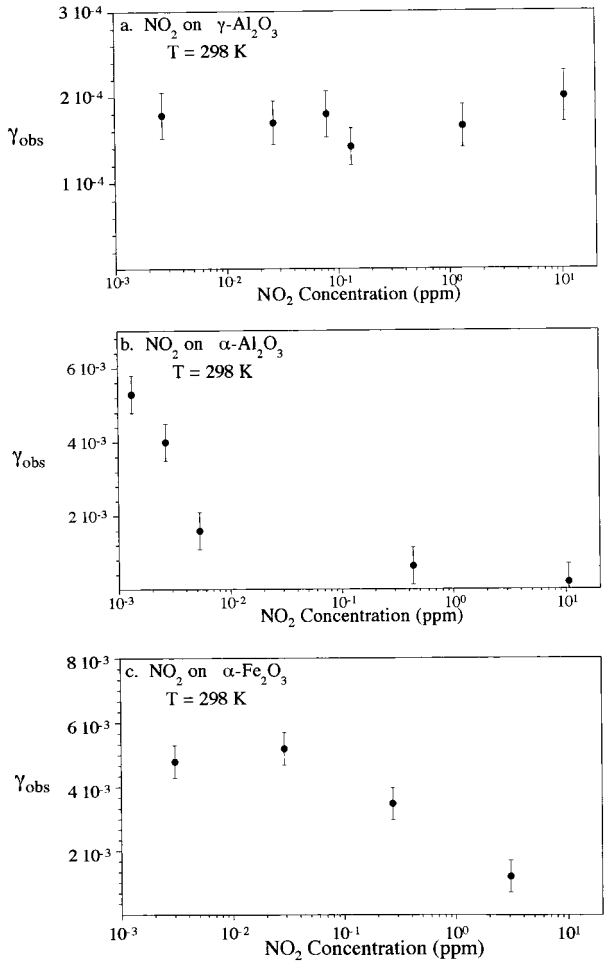

Figure 1. Observed initial uptake coefficient, γ_{obs}, for NO_2 on (a) γ-Al_2O_3, (b) α-Al_2O_3, and (c) α-Fe_2O_3 as a function of initial NO_2 pressure within the Knudsen cell. Error bars are ±15%. All sample masses were approximately 250 mg (1 ppm = 0.76 mTorr ≅ 2.4×10^{13} cm^{-3}).

In the next section, several examples are given that demonstrate the success as well as some of the difficulties in applying the KML model to experimental data. In addition, a new method is described that greatly simplifies the data analysis for powdered samples.

Results

Applications of the KML Model. In this section, the uptake of NO_2 on a variety of atmospherically relevant particle surfaces including mineral oxides (Al_2O_3 and Fe_2O_3) and carbon black are investigated using the KML model. The pressure dependence for the initial uptake coefficient of NO_2 on γ-Al_2O_3, α-Al_2O_3, and α-Fe_2O_3 is also examined.

The initial uptake coefficient for NO_2 on 250 mg samples of γ-Al_2O_3 is presented as a function of pressure in Figure 1a. The lack of any observable pressure dependence from 0.002 to 10 ppm corresponding to approximately 2 μTorr to 8 mTorr indicates that many more sites are accessible than would be possible if only the top layer were reacting. This suggests that the effective diffusion constant, and concomitantly the probe depth, is relatively large, which would indicate that the true uptake coefficient, γ_t, is very low as shown below.

As discussed in the previous section, the experimental variable in the KML model is the sample mass. The observed initial uptake coefficient for NO_2 on γ-Al_2O_3 is presented as a function of mass in Figure 2. Since there is no observable pressure dependence, over the experimentally accessible pressure range, the data were collected at a pressure of 0.100 mTorr to maximize signal levels while staying in the molecular flow regime. The results of the KML model, using $\tau = 3$ as suggested by previous work[7,11] and the physical parameters reported in Table 1, are presented in Figure 2. It can be seen that the model fits both the form and the absolute measured values exceptionally well. As predicted by the lack of any measurable pressure dependence, the true initial uptake coefficient, γ_t, is very small, 2.5×10^{-8}.

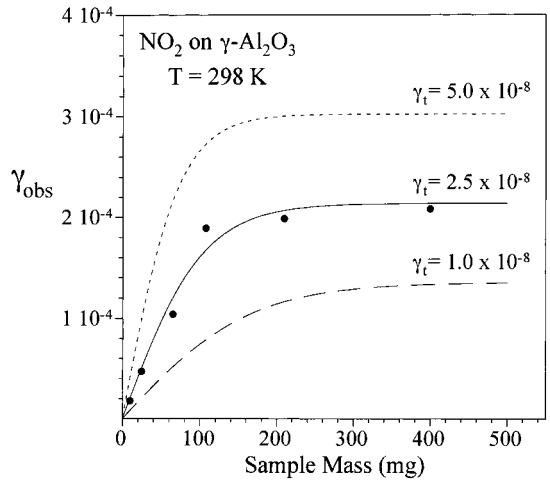

Figure 2. Observed initial uptake coefficient, γ_{obs}, for NO_2 on γ-Al_2O_3 as a function of sample mass. The filled circles represent experimental data, and the lines depict the KML model results using the physical properties listed in Table 1. The solid line is the best fit to the data, and the dashed lines are included to indicate model sensitivity.

Although the observed uptake coefficient for NO_2 on α-Al_2O_3 is almost identical to that of γ-Al_2O_3, at a pressure of 8 mTorr, the pressure dependence is strikingly different (Figure 1b). For the reaction of NO_2 on 250 mg samples of α-Al_2O_3, there is a clear pressure dependence, with lower pressures resulting in much larger observed uptake coefficients. This suggests that site blocking effects are significant down to the lowest experimental working pressures that we can achieve with a reasonable signal-to-background level. If site blocking is responsible for the decrease in observed reactivity at higher pressures, then there should be some pressure below which the observed reactivity is not pressure-dependent. Unfortunately, however, experimental limitations prevent our exploring pressures below 1 μTorr.

The mass dependence of the observed initial uptake coefficient for NO_2 on α-Al_2O_3 at a pressure of 2 μTorr is presented in Figure 3. When the KML model was applied to these data using a tortuosity value of 3, there was no good fit for any γ_t value. In fact, it was not possible to achieve a reasonable fit for any γ_t value over the expected range of possible τ values, 1−8. As such, γ_t and τ were varied independently and without constraint until the best fit was achieved. Although there is a concern that with two independent variables there will be no unique set of values that fit the experimental data, as discussed below, that does not appear to be the case here.

The results of the KML model are plotted with the experimental data in Figure 3 for three different γ_t values, 5.0×10^{-6}, 1.0×10^{-5}, and 2.5×10^{-5}. For each of these values, the tortuosity was adjusted to produce the best fit to the plateau region of the data. Of these, only the $\gamma_t = 1.0 \times 10^{-5}$ results also fit the low-mass data with any degree of success. The other model results are included to demonstrate that even for relatively small deviations in γ_t, large changes in the tortuosity are necessary to reproduce the experimental value of the plateau

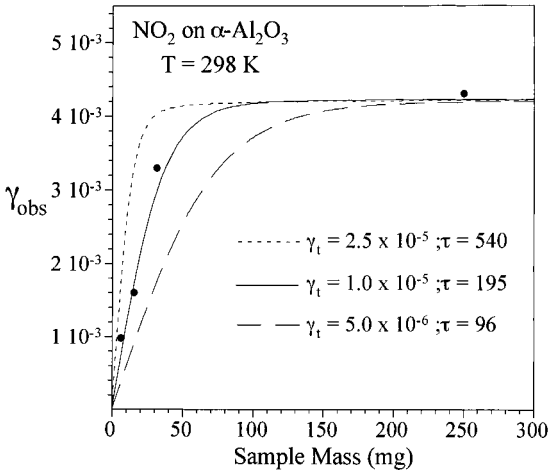

Figure 3. Observed initial uptake coefficient, γ_{obs}, for NO_2 on α-Al_2O_3 as a function of sample mass. The filled circles represent experimental data, and the solid lines depict the results of the KML model using the indicated γ_t and τ values. See text and Table 1 for additional modeling parameters.

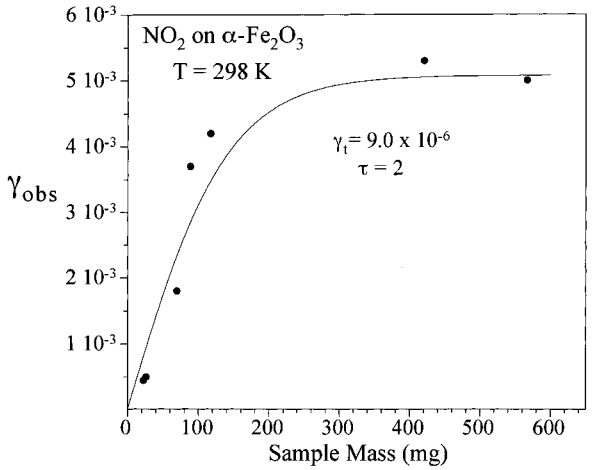

Figure 4. Observed initial uptake coefficient, γ_{obs}, for NO_2 on α-Fe_2O_3 as a function of sample mass. The filled circles represent experimental data, and the solid line depicts the results of the KML model using the physical properties listed in Table 1 and the indicated values for γ_t and τ.

region and even then there is substantial deviation from the experimental values for the lower masses. Though not shown, it is also possible to adjust τ to fit the low-mass data, but then the plateau value is significantly shifted from the experimental value. Thus, it appears that even though there are two independent adjustable variables in the model, there are two distinctly different portions of the data that need to be fit. As such, there is a unique set, or at least a relatively small range of γ_t and τ values that will successfully fit both the low- and high-mass regions of the experimental data. As demonstrated above, for the heterogeneous reaction of NO_2 on α-Al_2O_3 these values are 1.0×10^{-5} and 195 for γ_t and τ, respectively.

Large values of the tortuosity factor are not needed to model the heterogeneous reaction of NO_2 on α-Fe_2O_3. In these experiments, the pressure dependence of the observed uptake coefficient showed there was an initial increase of γ_{obs} followed by a leveling off below 20 μTorr (Figure 1c). Experiments were done at a gas-phase pressure of 2 μTorr. The observed initial uptake coefficient plotted as a function of α-Fe_2O_3 mass is shown in Figure 5. As can be seen, the best fit to the data is for γ_t of 9.0×10^{-6} using a tortuosity factor of 2. The wide variation

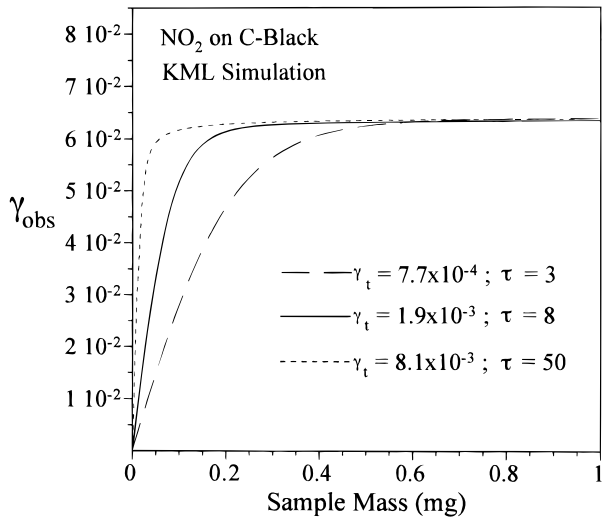

Figure 5. Application of the KML model for NO_2 on carbon black as a function of sample mass. The lines depict the results of the KML model for a range of γ_t and τ values, which yield a plateau value of $\gamma_{obs} = 0.064$ (see text). The relevant physical properties of carbon black are given in Table 1.

of τ for NO_2 diffusion through these oxide samples will be discussed.

We have also modeled results for NO_2 on carbon black as a function of mass. This system has been studied previously[12] and has a higher uptake coefficient than the mineral oxides. In addition, it has been reported that the observed uptake coefficient does not depend on sample mass. The model was run using the values in Table 1 with the tortuosity set equal to 3, 8, and 50. In each case, γ_t was adjusted until the plateau value of 0.064 was reached, in accordance with previously published work by Tabor, Gutzwiller, and Rossi.[12] The effect of increasing τ, and thus decreasing D_e, is demonstrated in Figure 5 where a larger tortuosity is associated with both a greater value for γ_t and a steeper mass dependence in the low-mass regime. Even for $\tau = 3$, the linear mass region does not extend much beyond 0.2 mg (for an 11.88 cm^2 sample holder). This explains why Tabor et al. did not observe any mass dependence.[12] In their experiments, by use of a sample holder of approximately the same size, the lowest sample mass used was approximately 25 mg, which is clearly on the plateau region where no mass dependence is expected. In fact, it would be nearly impossible to prepare a uniform sample of $\leq$0.2 mg of carbon black over the entire sample holder area of $\sim$10 cm^2. The limitation this places on the model is considered in more detail in the Discussion.

In general, nonideal gas behavior due to nonzero residence time is likely to be a significant problem in applying the KML model to systems with sticky reactants such as HNO_3. In addition, the internal structure within a given particle may affect diffusion by temporarily trapping a reactant molecule in an internal pore, thus reducing the effective diffusion constant. The extent of the internal structure for a given particle can be found by considering the ratio of the BET measured area of a single particle ((ρ_t)(particle volume)(S_{BET})) to the surface area of a sphere of the same average radius. On the basis of the properties listed in Table 1, these values turn out to be 1.0 for α-Fe_2O_3, 1.1 for γ-Al_2O_3, and 10 for α-Al_2O_3. Notably, the best fit values of τ reported here have a similar distribution, with $\tau = 2$, 3, and 195 for α-Fe_2O_3, γ-Al_2O_3, and α-Al_2O_3, respectively. Though not conclusive, this does suggest that particle morphology is at least partly responsible for the need to use high τ values to fit the data. In addition, the relationship between surface area

ratio and best fit τ values can be used to estimate a value of τ for carbon black. The surface area ratio for carbon black is 1.85, which, on the basis of the above data for γ-Al_2O_3, α-Fe_2O_3, and α-Al_2O_3 as well as data for γ-Fe_2O_3 (data not shown but values of $\tau = 20$ with a surface area ratio of 1.4), suggests a τ value of approximately 50. As will be shown in the Discussion, this value can be used to help determine the value of γ_t for the reaction of NO_2 on carbon black.

The above examples demonstrate that for heterogeneous reactions with a relatively low true uptake coefficient ($\leq 10^{-3}$), the KML model can reproduce experimental results quite well. However, the use of a calculated effective diffusion constant, D_e, as a fitting parameter through τ is a major weakness of the analysis, which is likely to invoke a certain amount of skepticism as to the accuracy of the resultant γ_t values, especially when the corrections to γ_{obs} are very large. It should be noted that if the effective diffusion constant could be measured, the tortuosity factor would not be needed and the only fitting parameter would be γ_t. This would enable the model to fit the plateau region uniquely with γ_t, eliminating the need to collect data over a wide mass range. Unfortunately, measuring D_e for reactive gases within powdered samples is not an easy task and there are very few reported values for relevant gas/powdered samples in the literature. As such, in the next section a simple method is developed that eliminates the use of the diffusion constant and tortuosity factor in the analysis of the true initial uptake coefficient, γ_t.

Linear Mass-Dependent (LMD) Regime. In each of the previous examples, the observed initial uptake coefficients and reaction probabilities, at very low sample masses, showed a very nearly linear mass dependence. In this low-mass range, the observed initial uptake coefficient calculated using eq 6 (or eq 7) is directly proportional to the sample mass. This arises because for very thin samples the probe or interrogation depth of the reactant gas molecules is greater than the depth of the powdered sample and the entire sample can be accessed. In this situation, the entire sample area contributes to the observed uptake coefficient and extracting the true uptake coefficient from the observed uptake coefficient requires consideration of both the entire reactive area and the resultant increase in the number of collisions a molecule makes within the depth of the powdered sample. As shown below, this leads to a very simple correction factor that will work for any reactant/substrate system for which this linear mass regime can be measured.

In the derivation of the equation for the observed uptake coefficient (eq 6 or 7), it is assumed that each time a gas-phase molecule approaches the sample it collides only once and only with the top layer. For porous samples with an uptake coefficient much less than unity both of these assumptions are wrong. The effect of multiple collisions on the topmost or external layer of particles can be accounted for by considering a roughness factor, which can be estimated from the ratio of the actual surface area to the projected surface area. For smooth spherical particles, this value will be $2\pi r^2/(\pi r^2) = 2$, and for "rough" particles it can be significantly higher. However, a potentially far more important consideration comes from the observation that in the linear region the incoming molecules can access all of the particles and a correction for the "internal" collisions in the lower layers of the powdered sample must also be found. In this way, the observed uptake coefficient, γ_{obs}, can be broken down into two components, one from the reaction with the external area, γ_e, and one from reaction with the internal surface area, γ_i. The situation is shown graphically in Figure 6.

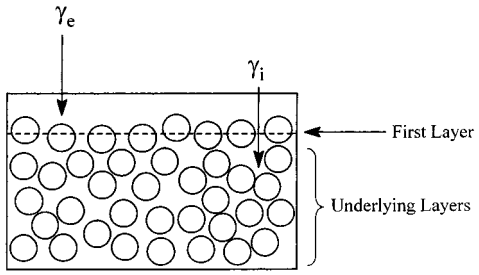

Figure 6. Graphical representation of a powdered sample in the sample holder of a Knudsen cell, demonstrating the external, γ_e, and internal, γ_i, contributions to the observed uptake coefficient, γ_{obs}.

The geometric area of the sample holder, A_s, is equivalent to the area of the top layer of particles projected onto the top layer plane, A_p, plus the area of the voids, A_v.

$$A_s = A_p + A_v \tag{14}$$

The ratio A_v/A_s is defined as the pore ratio X and is the fraction of the surface that is "open". It is equal to 9.3% for hexagonal close-packed particles and 21.5% for cubic close-packed particles. Frequently, however, especially for very small particles, neither close-packed arrangement is achieved and the surface pore ratio is even higher. Thus, it is not surprising that diffusion into the underlying layers is a facile and significant process. The net effect is that molecules that approach the surface are likely to enter the underlying layers where they will make many collisions with the sample before they are adsorbed or exit the sample. These extra collisions will significantly amplify the observed uptake coefficient. As shown below, extracting true uptake coefficients from observed uptake coefficients is then a matter of determining the amplification in γ_{obs} brought about by the extra collisions with the underlying layers.

Since the Knudsen cell dimensions are substantially less than the mean free path of the molecules in the chamber, homogeneous gas-phase collisions are extremely rare and can be neglected. This is known as the Knudsen flow regime, and under these conditions the average number of collisions a particle makes before exiting the cell, N, is independent of the cell's configuration and equal to the inverse of the fractional probability of colliding with the exit orifice. Thus, N is equivalent to the total interior surface area of the cell, A_{cell}, divided by the area of the escape aperture, A_h. Additionally, if there were more than one exit orifice, the areas would be additive and N would be equal to $A_{cell}/(A_{h1} + A_{h2} + A_{h3} + ...)$.

Since the dimensions of the interparticle void space are much smaller than those of the Knudsen cell and since the pressure inside these voids must be less than or equal to that in the cell, the gas flow inside the powdered sample must also be in the Knudsen flow regime. Therefore, the entire sample can be thought of as a virtual Knudsen chamber with the "holes" between particles in the top layer acting as exit apertures and the internal area acting as the cell walls. The average number of collisions, N, for a molecule in this virtual chamber will be

$$N = \frac{\text{total interior area of cell}}{\text{total void area of top layer}} \tag{15}$$

$$= \frac{A_{BET} - \left(\frac{1}{2}A_{top}\right) + A_s + A_{sw}}{XA_s} \tag{16}$$

$$\approx \frac{A_{BET}}{XA_s} \tag{17}$$

where A_{BET} is the total BET surface area ((S_{BET})(mass)), ($^1/_2$)(A_{top}) is the external area of the topmost layer, A_s is the area of the bottom of the sample holder, A_{sw} is the covered area of the sample compartment walls ((sample depth)($2\pi R$)), and XA_s is the void area A_v. The simplifications made in going from eq 16 to eq 17 arise because the BET area is in general much greater than the other areas.

With the average number of collisions known, the relationship between γ_t and γ_{obs} can be derived. As an experiment starts, the number of gas-phase molecules in the cell has reached steady state and the flow of reactant molecules into the cell is equal to the flow out of the cell through the exit orifice. This can be expressed as

$$F = k_{esc} n_o \tag{18}$$

where F is the flow into the cell, k_{esc} is the escape rate constant, and n_o is the steady-state number of gas molecules in the cell prior to opening the sample compartment.

When the sample compartment is opened, the sample acts as an additional sink, causing the pressure to drop. As the active sites on the sample become blocked, the pressure will stop dropping and start to return to its original value. Temporarily then, the cell is again in steady state and the flow in is equal to the flow out plus the loss to the sample. This can be expressed as

$$F = k_{esc} n + k_e n + k_i n \tag{19}$$

In eq 19, n is the steady-state number of gas molecules in the cell with the sample compartment open and k_e and k_i are the reactive rate constants for loss to the external and internal sample surfaces, respectively.

Since the flow into the cell does not change during the experiment, eq 18 can be set equal to eq 19 to yield

$$k_e + k_i = k_{esc}\left(\frac{n_o - n}{n}\right) \tag{20}$$

Since the rate constants in eq 20 will vary with reactor geometry, it is convenient to express them in terms of the uptake coefficient through the following general equation,

$$\gamma_t = \frac{k}{\omega A N} \tag{21}$$

where k is a first-order rate constant (s^{-1}), ω is the flux of gas-phase molecules (s^{-1} cm^{-2}) to the area of interest, A (cm^2), and N is the average number of collisions the molecule makes with A. Solving eq 21 for k_{esc}, k_e, and k_i yields

$$k_{esc} = \omega A_h \tag{22}$$

$$k_e = \omega A_p 2\gamma_t \tag{23}$$

$$k_i = \omega A_v \frac{A_{BET}}{A_v}\gamma_t \tag{24}$$

In eq 22, for the exit orifice, N and γ have both been set equal to 1. For the external component, eq 23, A is equal to A_p and N has been set to $2\pi r^2/(\pi r^2) = 2$. Similarly for the internal component, A is A_v and, as determined above, N is equal to $A_{BET}/(XA_s) = A_{BET}/A_v$. Now, substituting eqs 22−24 into eq 20 yields

$$\gamma_t = \frac{A_h}{2A_p + A_{BET}}\left(\frac{n_o - n}{n}\right) \tag{25}$$

Since $A_{BET} \gg A_p$ and n is directly proportional to the experimentally observable mass spectral intensity, I, eq 25 can be rewritten as follows,

$$\gamma_t = \frac{A_h}{A_{BET}}\left(\frac{I_o - I}{I}\right) = \left(\frac{A_s}{A_{BET}}\right)\gamma_{obs} \tag{26}$$

Equation 26 gives a simple correction factor with which the true uptake coefficient, corrected for multiple collisions with the entire BET sample area, can be extracted from the observed value, which assumes no diffusion into the underlying layers. Not surprisingly, the correction factor, like the number of collisions, scales with the BET area. It is interesting to note that both A_p and A_v cancel out during the derivation. This indicates that for the assumed experimental conditions of low uptake coefficient and sample mass in the linear regime, the packing geometry of the powder is unimportant.

Applications of the LMD Regime. The linear mass dependent regions of the observed uptake coefficients for NO_2 on γ-Al_2O_3, α-Al_2O_3, and α-Fe_2O_3 are presented in parts a, b, and c of Figure 7, respectively. In each case, the observed uptake coefficient using the geometric area is plotted along with a linear least-squares fit to the data of the form $y = mx$ so that the fit is forced through the origin. The resultant correlation coefficients are greater than 0.99 for γ- and α-Al_2O_3 and 0.97 for α-Fe_2O_3. Although efforts were made to precisely replicate experimental conditions such as pump-down time, background levels, and operating pressure for each experiment, the increased scatter for the α-Fe_2O_3 samples may indicate a dependence on one or a combination of some of these experimental factors.

For any given data point on the graphs in Figure 7, γ_t can be calculated from the known mass (and thus BET area) and eq 26. Alternatively, as was done here, the slope of the best fit can be used to determine the true uptake coefficient as follows,

$$\gamma_t = [\text{slope } (\text{mg}^{-1})]\frac{A_s\ (\text{cm}^2)}{S_{BET}\ (\text{cm}^2\ \text{mg}^{-1})} \tag{27}$$

By use of eq 27 and the measured S_{BET} values from Table 1 with the best fit slopes from Figure 7, γ_t values for γ-Al_2O_3, α-Al_2O_3, and α-Fe_2O_3 were calculated to be 2.0×10^{-8}, 9.3×10^{-6}, and 9.7×10^{-6}, respectively. As shown in Table 2, these values compare very well with the values obtained using the KML model.

The reaction of 2 μTorr of nitric acid with $CaCO_3$ was also investigated using the LMD regime. In these experiments, the sample cover is a polished aluminum disk that presses against a viton O-ring to seal the sample compartment. It was intentionally left uncovered by halocarbon wax to ensure a tight seal. For the NO_2 experiments, this surface did not contribute significantly to γ_{obs}, as evidenced by blank experiments in which no sample was added and no reaction could be discerned as well as by the zero y intercept values and high correlation coefficients in Figure 7. However, blank experiments with HNO_3 resulted in a very clear reaction with γ_{obs} equal to $\sim 1 \times 10^{-3}$. When the γ_{obs} values were corrected for contribution from the lid, the resultant values were found to be directly proportional to sample mass with a linear least-squares fit to the data yielding a slope of 1.6×10^{-5} and a correlation coefficient greater than

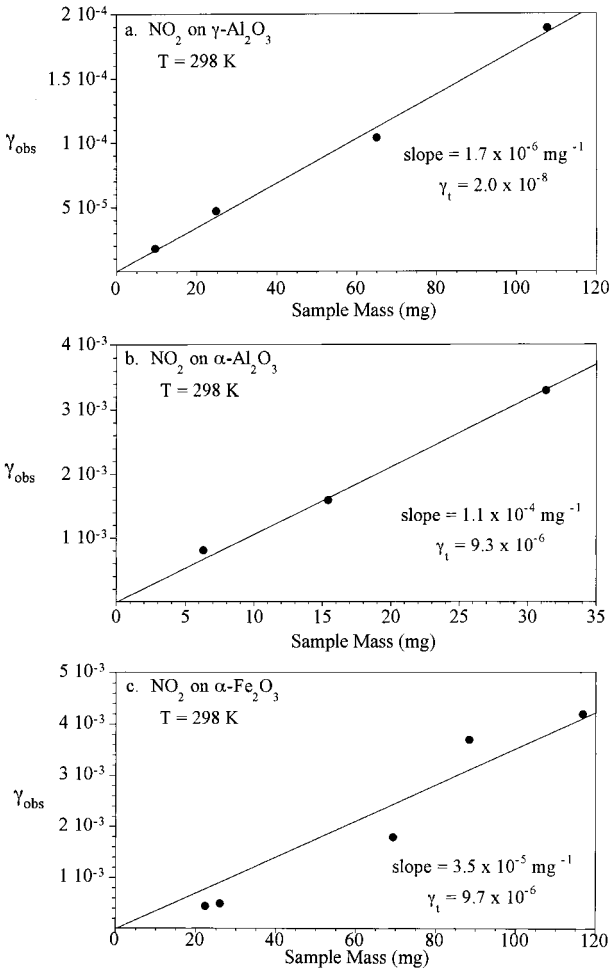

Figure 7. Linear mass-dependent regions of the observed uptake coefficient for NO_2 on (a) γ-Al_2O_3, (b) α-Al_2O_3, and (c) α-Fe_2O_3. The filled circles represent experimental data, and the solid lines are linear least-squares fits to the data with indicated slopes. The true uptake coefficients, γ_t, are calculated from the slopes of the lines and the specific BET surface areas of the powders using eq 27.

TABLE 2: Uptake Coefficients and Probe Depths Determined for Heterogeneous Reaction of NO_2 on Powdered Samples

	γ-Al_2O_3	α-Al_2O_3	α-Fe_2O_3	C-black
γ_{obs} (plateau)	2.1×10^{-4} [a]	4.2×10^{-3} [a]	5.1×10^{-3} [a]	6.4×10^{-2} [b]
$\gamma_{t\ (KML)}$ [c]	2.5×10^{-8}	1.0×10^{-5}	9.0×10^{-6}	8.1×10^{-3} [d]
$\gamma_{t\ (LMD)}$ [e]	2.0×10^{-8}	9.3×10^{-6}	9.7×10^{-6}	
probe depth[f] (layers)	15000	32	264	3.5
probe depth[g] (mass)	113 mg	34.4 mg	139 mg	0.016 mg

[a] This work. [b] Reference 12. [c] γ_t determined using the KML model. [d] Determined using $\tau = 50$ (see text for further details). [e] γ_t determined using the LMD regime. [f] Calculated from $\eta \times$ (total number of layers) in the plateau region. [g] Calculated using the probe depth in layers and the parameters in Table 1.

0.99. These data are plotted in Figure 8. By use of eq 27 and a measured S_{BET} value of 14 $cm^2\ mg^{-1}$, γ_t is found to be 1.4×10^{-5}.

The reaction of acetone with TiO_2 at a pressure of 2 μTorr is given as another example of a heterogeneous reaction analyzed in the LMD regime. Only two data points were obtained for this reaction, since this is the minimum number of data points needed to establish that γ_{obs} is directly proportional to mass. Of course any two points will yield a line; however, to be in the linear regime, γ_{obs} must scale directly with sample surface area (or sample mass). For 3 and 8 mg samples the γ_{obs} values were 0.047 and 0.12, respectively, indicating that these masses

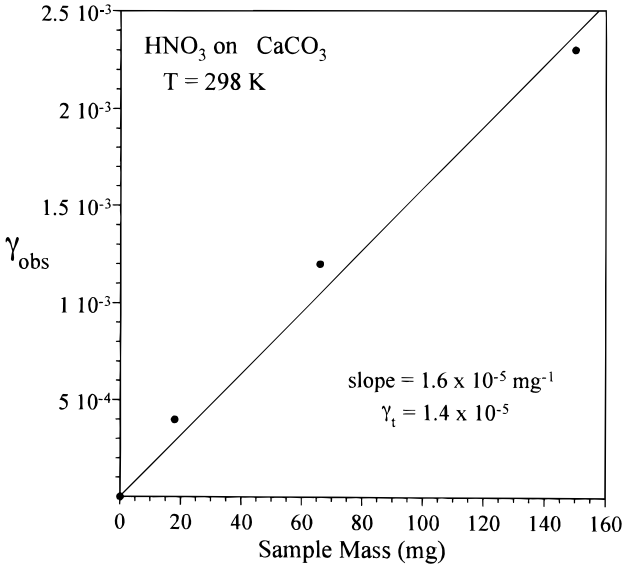

Figure 8. Linear mass-dependent region of the observed uptake coefficient for the reaction of HNO_3 on $CaCO_3$, corrected for reaction with the lid (see text for details). The filled circles represent experimental data, and the solid line is the linear least-squares fit to the data. The value of γ_t is calculated from the slope and the specific BET surface area of the $CaCO_3$ powder using eq 27.

are in the linear regime. By use of eq 26 and the data given in Table 1 for the BET surface area, γ_t values of 3.7×10^{-4} and 3.6×10^{-4} for 3 and 8 mg, respectively, are determined. The very small deviation in γ_t values lends support to their accuracy and also serves as a further demonstration that the masses are in the linear regime.

Discussion

Importance of Reactant Pressure. With the exception of γ-Al_2O_3 the pressure-dependent studies showed higher uptake coefficients for lower pressures. Because the chemistry has been shown to be very similar for both γ- and α-Al_2O_3,[21] it is unlikely that differences in the kinetic order of the reaction on these two different Al_2O_3 particles are responsible for the observed behavior. In addition, the observation of higher γ_{obs} values at lower pressures is qualitatively consistent with site blocking or limited accommodation as being the causal factor. Because γ-Al_2O_3 has such a small γ_t and concomitantly a large probe depth, the effect is minimized. Presumably at high enough pressures, the observed uptake coefficient would decrease for this reaction as well. In any case, the strong dependence of uptake coefficients on pressure for the other species makes it clear that the pressure dependence of the uptake coefficient needs to be considered before any reported values are incorporated into atmospheric chemistry models.

Importance of Multiple Collisions in Powdered Samples. It is important to note that multiple collisions in the underlying layers of a porous sample can cause an amplification of the observed uptake coefficient. This amplification will cause the observed uptake coefficient to appear many times larger than its true value. Thus, the lower limit of uptake coefficients that can be measured for powdered samples is actually even lower than previously indicated.[2] Because the net amplification or correction factor for a given system is ultimately dependent on the probe depth, it is useful to consider some of the factors that affect it and how they impact the heterogeneous reactions studied here.

The probe depth is intimately related to the effectiveness factor η and is essentially the amount of sample that can be

accessed on the data acquisition time scale. The probe depth, in terms of layers of sample, is simply η times the total number of layers. Through η, the probe depth is dependent on the relative rates of reaction, γ_t, and diffusion into the underlying layers of the sample, D_e. It is important to note that in this case D_e is a measure of diffusion *around* individual particles and not *into* them and that probe depth refers to layers and not distance. Thus, for a given D_e, a larger γ_t will result in a smaller probe depth. Though convoluted in that D_e is not constant in these systems, this effect is clearly demonstrated in Table 2 as well as Figures 2−5. From the table it is clear that as the uptake coefficient decreases the probe depth dramatically increases. Inspection of Figures 2−5 reveals the same effect in that the extent of the linear region is greatly enhanced as γ_t decreases. Additionally, an increased probe depth results in a greater correction factor, which means that a reaction with a much smaller true uptake coefficient may not have a much smaller observed uptake coefficient. This can be seen in Table 2 where for γ- and α-Al_2O_3 γ_t values differ by a factor of ∼450 but γ_{obs} values only differ by ∼20.

One of the limitations of the analysis of the data for powdered samples is that the uptake coefficient must be small enough to allow the probe depth to exceed the physical limitations of sample preparation. This will of course be sample-dependent but from the heterogeneous reactions studied here appears to put the upper limit for γ_t that can be accurately measured with either of these models to be on the order of 10^{-3}. Where γ_t is greater than 10^{-3}, as was observed for the reaction of NO_2 on carbon black, another method must be used to find the true uptake coefficient. One possibility comes from the estimation of τ based on the BET-to-particle geometric surface area ratio. As discussed earlier, this suggests a τ value of 50 for carbon black, which in turn indicates a probe depth of 3.5 layers (73 cm^2). Using this as the surface area in eq 26 yields a γ_t value of 9×10^{-3}, and this is the value reported in Table 2. As discussed above, owing to the physical limitations of sample preparation, the accuracy of our estimation cannot be tested at this time.

Use of the BET Surface Area. One of the assumptions made in the derivation of *N*, the average number of collisions a molecule makes with the powdered sample, was that the entire BET area was accessible. In general the BET surface area is determined using molecular nitrogen because N_2 is small and unreactive. Therefore, molecular nitrogen is able to access the entire particle surface, including any fissures or pores with dimensions as small as a few angstroms. Although this yields an accurate determination of the surface area, there is some question as to whether all of that area is available to larger, more reactive molecules. The extent to which this could be a factor can be gained from the previously calculated BET to particle geometric surface area ratios: 1.0 for α-Fe_2O_3, 1.1 for γ-Al_2O_3, 1.85 for carbon black, and 10 for α-Al_2O_3. These values indicate that, with the exception of α-Al_2O_3, even if the entire internal structure is inaccessible to the reactant molecules, use of the particle geometric area instead of the BET surface area in determining γ_t would be relatively small. For α-Al_2O_3, the available surface area could differ by as much as an order of magnitude, which would increase γ_t by the same amount. (Note that the particle geometric area is not the same as the geometric area of the sample holder discussed previously but is the same as the total spherical area calculated from the average radius of the particles.)

Suggested Experimental Protocol for Measuring Heterogeneous Reactions on Solid Particle Surfaces Using a Knudsen Cell Reactor. In light of the results and analysis presented here, the following experimental protocol is suggested for Knudsen cell studies of heterogeneous reactions on powdered samples.

(1) Pressure-dependent measurements should be made at a variety of pressures. The sample mass used for these experiments should be relatively high to minimize any mass-dependent effects.

(2) The BET surface area of the powdered sample should be measured as well as the particle diameter so that the particle geometric area can be determined. This information is needed in order to determine γ_t from the Knudsen cell data.

(3) Mass-dependent measurements should be made at a given pressure, if possible at the lowest possible pressure. If a linear mass dependence for γ_{obs} is observed, the entire sample surface area should be used to determine γ_t. If the system is too reactive and a linear mass regime cannot be experimentally accessed, γ_t should be determined using the surface area of the probe depth (if this can be determined or estimated). If there is no way to estimate the probe depth, it is recommended that γ_{obs} be reported as an upper limit to γ_t.

Even if this protocol is followed, there are likely to be other difficulties if the reaction being studied is more complex than a simple adsorption process. It is becoming increasingly clear that water can play an important role in the heterogeneous chemistry of particulate aerosols[13,22−25] and is shown to be important in the heterogeneous reaction of HNO_3 on NaCl particles.[13,23−25] The amount and distribution of water on the particle surface will have an effect on the surface area available for reaction. Until the effective area or probe depth for the salt particles with adsorbed water is known, it will be difficult to determine an accurate value of γ_t for the HNO_3−NaCl reaction.

Conclusions

A comprehensive discussion of the analysis of Knudsen cell data in determining the initial uptake coefficient for heterogeneous reactions involving gas−solid reactions on powdered solids has been given. The main conclusion of this work is that, in general, the use of the geometric sample holder area in determining the uptake coefficient is probably not justified in these systems. The Keyser−Moore−Leu model can be used to account for gas diffusion into the underlying layers of the powder. However, the use of the model is hindered by the fact that the diffusion constant for gases in powders is usually not known and difficult to measure. Another approach discussed here is one that takes advantage of the sample mass range in which the observed initial uptake coefficient is linearly proportional to the entire sample surface area and thus the sample mass. In this linear mass regime, the entire sample area is accessible for reaction and the true initial uptake coefficient can be determined by correcting the observed initial uptake coefficient for the resulting increase in the number of collisions that the average reactant molecule makes with the sample. The number of collisions is shown to be proportional to the entire surface area of the powdered sample, which is taken as the total BET area. Thus, only two experimental quantities are needed in order to determine γ_t: the sample mass and the BET area of the sample. However, the limitation of this approach appears to be that for heterogeneous reactions greater than 10^{-3} the linear mass regime may be difficult to measure. Finally, it is recommended that the pressure dependence of the observed initial uptake coefficient be considered over as wide a range as possible.

Acknowledgment. The authors gratefully acknowledge the National Science Foundation (Grant CHE-9614134) and the Camille and Henry Dreyfus Postdoctoral Program in Environ-

TABLE 3

number of collisions	apparent uptake coefficient
1	$\gamma_1 = \gamma_t$
2	$\gamma_2 = \gamma_1 + (1 - \gamma_1)\gamma_t$
	$= \gamma_t + (1 - \gamma_t)\gamma_t$
3	$\gamma_3 = \gamma_2 + (1 - \gamma_2)\gamma_t$
	$= \gamma_t + (1 - \gamma_t)\gamma_t + (1 - \gamma_t)^2\gamma_t$
N	$= \gamma_t \sum_{i=0}^{i=N-1} (1 - \gamma_t)^i$
	$= \gamma_t \frac{(1 - \gamma_t)^N - 1}{(1 - \gamma_t) - 1}$
	$= 1 - (1 - \gamma_t)^N$

mental Chemistry for support of this research. The authors thank Angela Goodman for the TEM measurements of the oxide particles.

Appendix

With the number of gas−solid collisions known, the relationship between the observed uptake coefficient, γ_{obs}, and the true uptake coefficient, γ_t, was derived from a kinetic approach in the body of the text. The same result can be derived from a more rigorous collision-by-collision approach as follows. The cumulative effect of multiple collisions for a given reactant molecule can be seen in Table 3 in which each successive collision adds to the observed uptake coefficient by the amount γ_t times the fraction of colliding molecules that have not reacted during all the prior collisions.

Thus, the contribution to the observed uptake coefficient, due to internal collisions, can be written as

$$\gamma_i = 1 - (1 - \gamma_t)^N A \tag{A1}$$

So that now

$$\gamma_{obs} = \gamma_e + \gamma_i \tag{A2}$$

$$= 2(1 - X)\gamma_t + X[1 - (1 - \gamma_t)^N] \tag{A3}$$

where X is the ratio A_v/A_p as discussed previously. However, when $\gamma_t \ll 1$, $(1 - \gamma_t)^N \approx 1 - N\gamma_t$ so that

$$\gamma_{obs} = 2(1 - X)\gamma_t + XN\gamma_t \tag{A4}$$

$$= \left(2(1 - X) + \frac{A_{BET}}{A_s}\right)\gamma_t \tag{A5}$$

Usually, $A_{BET}/A_s \gg 2$ so that

$$\gamma_t = \left(\frac{A_s}{A_{BET}}\right)\gamma_{obs} \tag{A6}$$

The restriction that γ_t is much less than 1, which arises from the approximation made for the binomial expansion between eqs A3 and A4, appears to put an upper limit on the sample mass (through N). However, the prior constraint that the sample must be in the linear regime is more severe (i.e., has a higher order mass dependence), which is to say that if the sample is in the linear regime, then the approximation $(1 - \gamma_t)^N \approx 1 - N\gamma_t$ must be valid and introduces no extra constraints on the experiment.

References and Notes

(1) Golden, D. M.; Spokes, G. N.; Benson, S. W. *Angew, Chem., Int. Ed. Engl.* **1973**, *12*, 534.

(2) Caloz, F.; Fenter, F. F.; Tabor, K. D.; Rossi, M. J. *Rev. Sci. Instrum.* **1997**, *68*, 3172.

(3) Colussi, A. J.; Amorebieta, V. T. *J. Phys. Chem.* **1995**, *99*, 13921.

(4) Golden, D. M.; Manion, J. A.; Reihs, C. M.; Tolbert, M. A. In *The Chemistry of the Atmosphere: Its Impact on Global Change*; Calvert, J. G., Ed.; Blackwell Scientific Publications: Oxford, U.K., 1994.

(5) DeMore, W. B.; Sander, S. P.; Golden, D. M.; Hampson, R. F.; Kurylo, M. J.; Howard, C. J.; Ravishankara, A. R.; Kolb, C. E.; Molina, M. J. *Chemical Kinetics and Photochemical Data for Use in Stratospheric Modeling*; JPL Publication 97-4; Jet Propulsion Laboratory: Pasadena, CA, 1997.

(6) In this context, the term "uptake coefficient" refers to the net loss to the sample, which may include both adsorption and reaction on the surface. Though the latter is more formally termed the "reaction probability", no such distinction is made here, so "uptake coefficient" is used throughout the text.

(7) Keyser, L. F.; Moore, S. B.; Leu, M.-T. *J. Phys. Chem.* **1991**, *95*, 5496.

(8) Hanson, D. R.; Ravishankara, A. R. *J. Phys. Chem.* **1992**, *96*, 2682.

(9) Keyser, L. F.; Leu, M.-T.; Moore, S. B. *J. Phys. Chem.* **1993**, *97*, 2800.

(10) Hanson, D. R.; Ravishankara, A. R. *J. Phys. Chem.* **1993**, *97*, 2802.

(11) Fenter, F. F.; Caloz, F.; Rossi, M. J. *J. Phys. Chem.* **1996**, *100*, 1008.

(12) Tabor, K.; Gutzwiller, L.; Rossi, M. J. *J. Phys. Chem.* **1994**, *98*, 9801.

(13) Beichert, P.; Finlayson-Pitts, B. J. *J. Phys. Chem.* **1996**, *100*, 15218.

(14) Underwood, G. M.; Miller, T. M.; Grassian, V. H. *J. Phys. Chem. A* **1999**, *103*, 6184.

(15) Dushman, S. *Scientific Foundations of Vacuum Technique*, 2nd ed.; Wiley: New York, 1962.

(16) King, D. A.; Tompkin, F. C. *Trans. Faraday Soc.* **1968**, *64*, 496.

(17) Ho, F. G.; Strieder, W. *J. Chem. Phys.* **1982**, *76*, 673.

(18) Lee, P. H.; Kozak, J. J. *J. Chem. Phys.* **1987**, *86*, 4617.

(19) Burganos, V. N.; Sotirchos, S. V. *Chem. Eng. Sci.* **1989**, *44*, 2629.

(20) Currie, J. A. *J. Appl. Phys.* **1960**, *11*, 318.

(21) Underwood, G. M.; Miller, T. M.; Grassian, V. H. Unpublished results.

(22) Goodman, A. L.; Underwood, G. M.; Grassian, V. H. *J. Phys. Chem. A* **1999**, *103*, 7217.

(23) Davies, J. A.; Cox, R. A. *J. Phys. Chem. A* **1998**, *102*, 7631.

(24) Ghosal, S.; Hemminger, J. C. *J. Phys. Chem. A* **1999**, *103*, 4777.

(25) Weis, D. D.; Ewing, G. E. *J. Phys. Chem. A* **1999**, *103*, 4865.